Arabian Journal of Geosciences (2019) 12: 284
https://doi.org/10.1007/s12517-019-4468-z

ORIGINAL PAPER

The depositional evolution and internal sedimentary architecture of a flood event-dominated experimental alluvial fan

Wenjie Feng[1] · Shenghe Wu[2] · Junling Liu[1] · Changmin Zhang[1] · Yanshu Yin[1] · Taiju Yin[1]

Received: 12 December 2018 / Accepted: 1 April 2019 / Published online: 23 April 2019

Abstract

In this article, based on a flume tank experiment, we attempt to provide some key insights to the depositional process and geomorphological evolution of an experimental alluvial fan dominated by flood events. In the experiment, all boundary conditions were kept constant besides the sediment and water supply in each flood event. The experimental fan formed after 12 flood events. The elevation at the observation points was measured and the geomorphology evolution during the whole experiment was recorded by time-lapsed digital images. It is showed that the depositional process of the experimental fan could be subdivided into three stages, including the sheet flood-dominated stage, the unconfined channel-dominated stage, and the confined channel-dominated stage. The spontaneous evolution of the experimental fan was indicated to be controlled by the continuously occupation of the accommodation space and resulted in the three-layer sedimentary architecture. With the growth of this experimental fan, the increasing rate of fan area and the vertically aggradational rate decreased. Meanwhile, the roughness of the fan edge changed from rapid fluctuation to gradually decrease.

Keywords Flood event-dominated alluvial fan · Autogenic · Flume experiment · Depositional evolution · Sedimentary architecture · Geomorphology

Introduction

Alluvial fan is a type of complex terrestrial sedimentary system that commonly developed at the margin of basins (Bull 1977; Al-Sarawi 1988; Stanistreet and McCarthy 1993; Brierley et al. 1993; Blair 1999a, 1999b). As for the alluvial fans, their depositional evolution, internal sedimentary architecture, and the reservoir configurations have received numerous concerns worldwide (Hooke 1967; Le Hooke and Rohrer 1979; Sorriso-Valvo et al. 1998; Clarke et al. 2010; Straub and Esposito 2013; Delorme et al. 2018).

The piedmont setting of alluvial fans where the feeder channel of an upland drainage basin intersects the mountain front assures that catastrophic fluid gravity flows and sediment gravity flows, including sheet floods, rock falls, rock slides, rock avalanches, and debris flows, are major constructional processes, regardless of climate (Blair and McPherson 1994). Braided river and low sinuosity/meandering river also play an essential role on the formation of alluvial fans (Stanistreet and McCarthy 1993). Sedimentary process of alluvial fan is controlled alternately by flood periods and inter-flood periods. Although the hydrodynamics and the depositional characteristics are severely complex, floods are usually characterized by rapid spring snowmelt, intense summer thunderstorms, or prolonged rainfall from moist air masses (Blair 2001). Fan deposits can be subdivided into two types, those resulting from streamflow and those resulting from debris flow and related processes (Nilsen 1982). Streamflow deposits behave in transport as essentially Newtonian fluids, whereas debris flow and related deposits behave in transport as more viscous fluids (Nilsen 1982). Debris flow was generally driven by flood events and occurs during flood peak periods, whereas the streamflow deposits predominantly occur at early and late stage of flood events. Therefore, many fans are composites of stream and debris flow sediment, and flood event is one of the dominant factors to construct and reshape/transform an alluvial fan (National Research Council 1996). However, studies

Editorial handling: B. Badenas

✉ Wenjie Feng
fengwenjie1017@163.com

[1] School of Geosciences, Yangtze University, Wuhan, China

[2] State Key Laboratory of Petroleum Resource and Prospecting, College of Geosciences, China University of Petroleum (Beijing), Beijing, China

concerned the depositional evolution and internal sedimentary architecture of flood event-dominated fan are very limited.

Although, much efforts have been performed on alluvial fan sedimentology investigations based on outcrops/subsurface records (Lin et al. 2018; Moscariello 2018; Nichols 2018; Chen and Guo 2017; Goswami 2017; Ielpi and Ghinassi 2016; Muravchik et al. 2014; Chakraborty and Paul 2014; Trendell et al. 2013; Fidolini et al. 2013; Yin et al. 2013; Sáez et al. 2007; López-Gamundí and Astini 2004; Ramos et al. 2002; Weissmann et al. 2002; Blair 2000; Stanistreet and McCarthy 1993; Ridgway and Decelles, 1993, b; Heward, 1978; DeCELLES et al., 1991; de Gibert and Sáez, 2009) and modern fans (Singh et al., 1993; Shukla et al., 2001; Bahrami, 2013; Davidson et al., 2013; Fontana et al., 2014; Ettinger et al., 2014; Latrubesse, 2015; Sahu et al., 2015; Zhang et al., 2015; Galve et al., 2016; Lu et al., 2018; Majumder and Ghosh, 2018). The process and effects of flood events during the formation of an alluvial fan still remain poorly understood (van der Meulen, 1986; National Research Council, 1996; Blair, 2000, 2001). The sedimentary evolution and associated internal architecture of flood event-dominated alluvial fans is often hampered by limited outcrops/subsurface data due to their poor filed preservations (Clarke et al., 2010). For example, time scales of modern alluvial fan formation are commonly too long to allow real-time observations to be made over a sufficient time period (Clarke et al., 2010). In contrast, the experimental physical modelling could provide detailed information for the geomorphology evolution and associated internal architecture construction (Le Hooke and Rohrer, 1979; Whipple et al., 1998; Clarke et al., 2010; Wang et al., 2015; Clarke, 2015; Zhang et al., 2016; de Haas et al., 2016; Delorme et al., 2016; Mouchené et al., 2017). In the past decade, the experimental models have been successfully applied for alluvial fan studies by numerous researchers, which have given insightful indications for their depositional evolution (Nilsen, 1982; Van Dijk et al., 2009; Clarke et al., 2010; Straub and Esposito, 2013; Straub and Wang, 2013; Guerit et al., 2014; Clarke, 2015).

To further develop our understanding of the sedimentary process and associated internal architecture of the flood event-driven alluvial fans, a physical experiment is performed in this paper. Aiming at the spontaneously sedimentary process and evolution without the constrain of extrinsic conditions, 12 identical flood events are planned to feed the experimental fan. In each flood event, water and sediments are supplied changing with the simulation time to reproduce the realistic flood process in nature. The surface morphology of the fan was recorded by time-lapsed digital cameras and the elevation was measured at the end of each flood event within a designed grid. The relevant evolution pattern of the fan was obtained by an integrated analysis of digital images and the elevation data. Internal architecture of the experimental fan was anatomy through sliced sections along both transverse and longitudinal directions.

Experimental design

According to the sedimentary conditions of flood event-dominated alluvial fan, a simulation device was set up (Fig. 1). The entire device includes a console, a feeder channel, a plan deposition area, and a water storage tank. The function of the console is to continuously agitate and release the sediments and water and transport the sediments to the deposition zone through the feeder channel. In order to reduce the influence of the control valve on flow speed, the feeder channel was designed as long as 2.5 m in length (Fig. 1). The deposition area is 4.5 m long and 3 m wide. The water storage tank is used to receive the water flowing out of the alluvial fan in order to prevent the deposits ponding. The geomorphology was recorded by time-lapsed digital cameras (Fig. 1).

In the experiment, external conditions were kept constant so that the experimental alluvial fan is formed spontaneously under the constant boundary conditions. In order to simulate the autogenic/spontaneous deposition process of alluvial fans in arid areas in natural environment, water and sediments are provided periodically to simulate flood events. It should be noted that the flood process is event-dominated. Although there is a change in flow and sediment flux during each flood process, the geological history of the entire alluvial fan, its hydrodynamics, sediment supply rate, and sedimentation could be considered to be approximate stable. Therefore, the experimental scheme can not only simulate flood events but also maintain the overall stability of the external conditions during the deposition process of the experimental alluvial fan.

Throughout the whole experiment, 12 flood events have been simulated. The boundary conditions of each flood event are listed as follows. A flood event can be divided into a high-fluidity period and a following low-fluidity period (Fig. 2). The high-fluidity period took 2 min and the later low-fluidity period took 4 min. The break between two adjacent flood events took 4 min. The peak water discharge (Q_W) was set as 2.0 l/s (Fig. 2a). The amount of sediment supply (Q_S) during every debris flow-dominated stage was 0.25 m^3 (dry sediments). During every stream-dominated stage, the sediment supply was 0.15 m^3 (dry sediments). Sediment supply was changed every half minutes and was associated with the discharge (Fig. 2b). In every flood event, no dry sediment was supplied in the last half minute of the duration of water supply. That was because the water discharge in the last half minutes was too low to transport sediment. The sediment supply was changed. The median particle size of the mixed sediments is about 350 μm, and the sediments mainly consist of fine sand, medium sand, and coarse sand, and contain a small amount of mud, silt, and gravel (Fig. 3).

To record the elevation of fan surface at the end of each flood event, a measure point network has been planned within an 11 × 21 grid. The interval of measurement points along x direction was 20 cm, and along y direction was 25 cm. At the

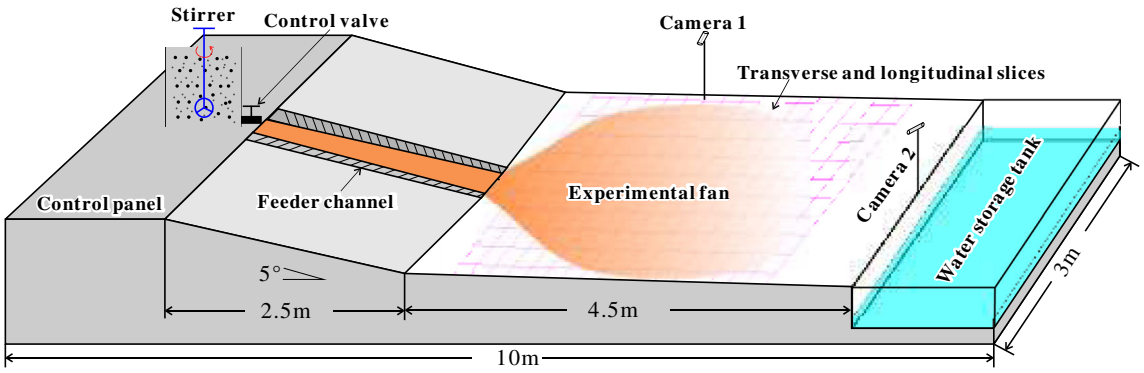

Fig. 1 Diagram of the facility used in experiment

end of each flood event, an elevation gird could be measured through a probe. The probe was a straight steel needle with a diameter of 1 mm. Inserting this probe into the deposit does not cause significant destruction on the deposited fan. At each measurement point, we measure the thickness of sediment for three times or more and take the average value as the final measured values. The bedform was considered as the reference surface with an elevation of zero. Therefore, the measured thickness was the elevation. In addition, the edge of the experimental fan would be measured in detail. A set of supplemental edge points would be measured with a small separation distance.

One longitudinal and 14 transverses section have been sliced after the experiment (Fig. 4). Observation on slices associated with the elevation of fan surface was utilized to analyze the distribution of coarse to fine sediments and the internal architecture of the experimental alluvial fan.

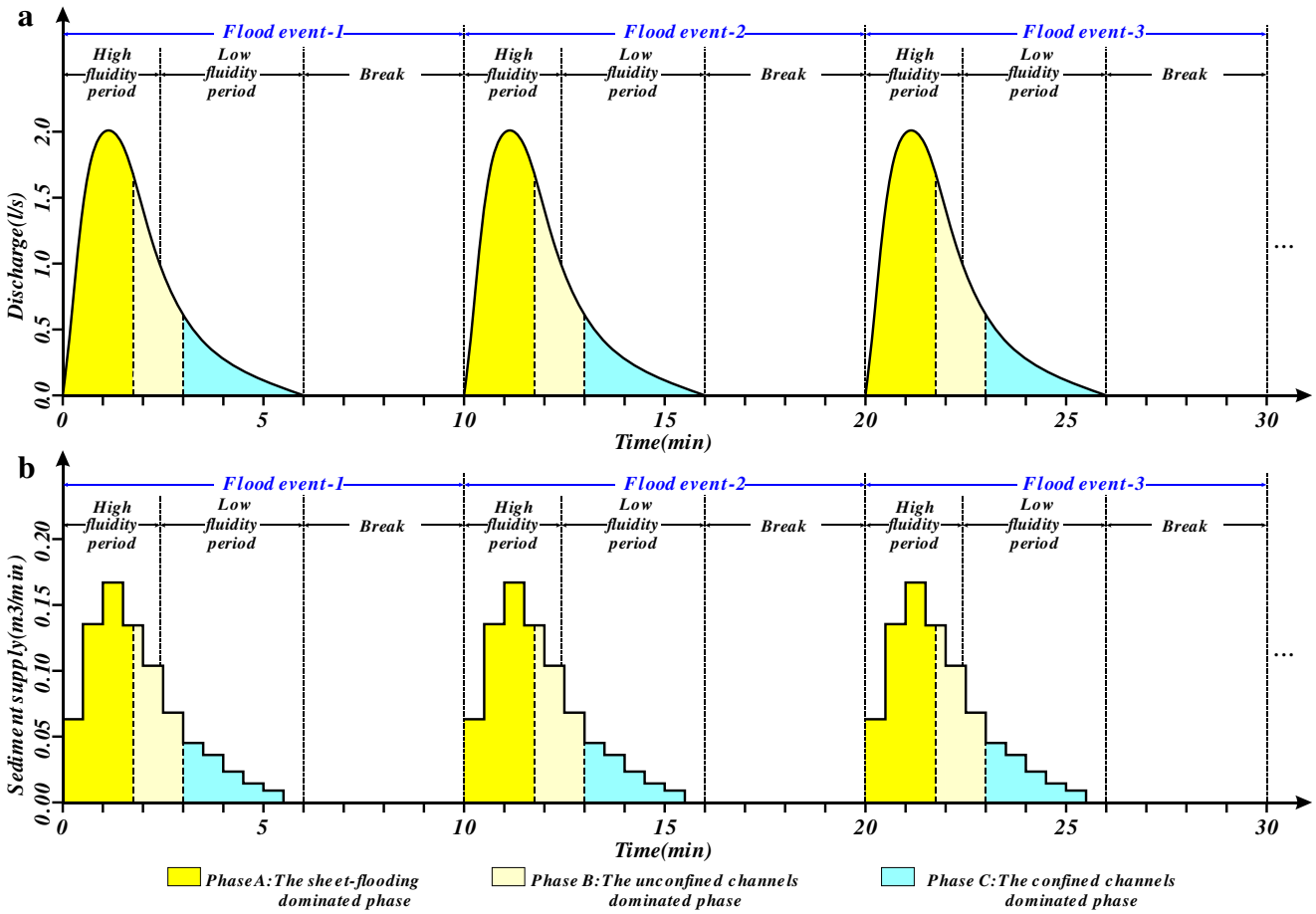

Fig. 2 Water discharge and sediment supply during the first three flood events. **a**. water discharge during the first three flood events; **b**. Sediment supply during the first three flood events

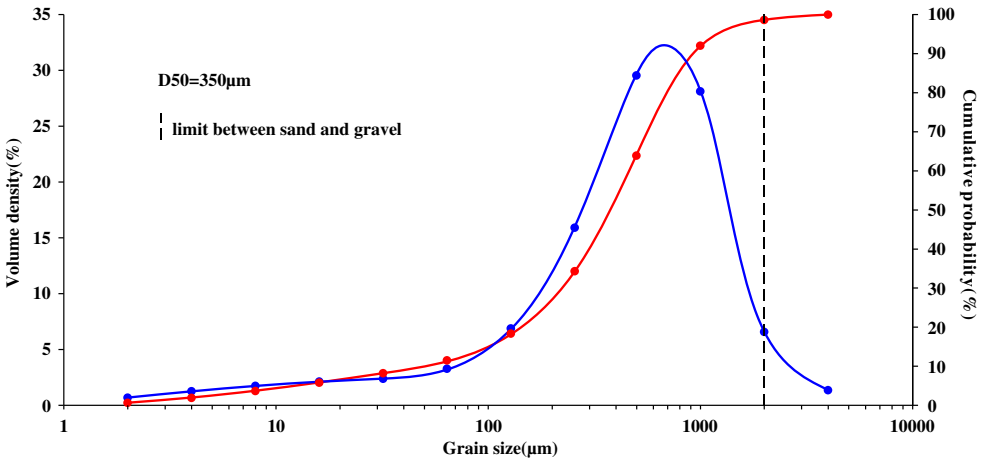

Fig. 3 Grain size of the mixed sediment used in the experiment

To investigate the growth law of fan surface, seven points (Fig. 4) distributed along the source direction were selected to record their elevation at the end of each flood event. Changes on fan surface elevation were analyzed by plotting the curves of elevation evolution for each point planned.

Observations of the flood event-dominated experimental alluvial fan

The depositional evolution of the alluvial fan during a flood event

Flood events are the main mechanism during the formation process of alluvial fan in arid to semi-arid climates. In a typical flood event, the flood is usually coming at the end of the rainfall process. The flood discharge will increase rapidly to its peak and gradually decrease to a low degree and the low-intensity water flow will last a relatively long time (Fig. 2). A large amount of sediments will be transported to the open area in the front of the mountain. Because the ability of current to transport sediments is positively correlated with its intensity, the main sedimentation occurs during the flood peak period. On the contrary, there is nearly no sediments deposited at fan surface because of the low flow intensity between two adjacent flood events. Therefore, sedimentation during a flood event can be regarded as a large-scale and isochronous architecture element in an alluvial fan.

The ability of sediment transportation and depositional rate is sensitive to the variation of water discharge. Therefore, flow and sedimentation on fan surface were changing with the discharge of water during a flood event. According to the observation on

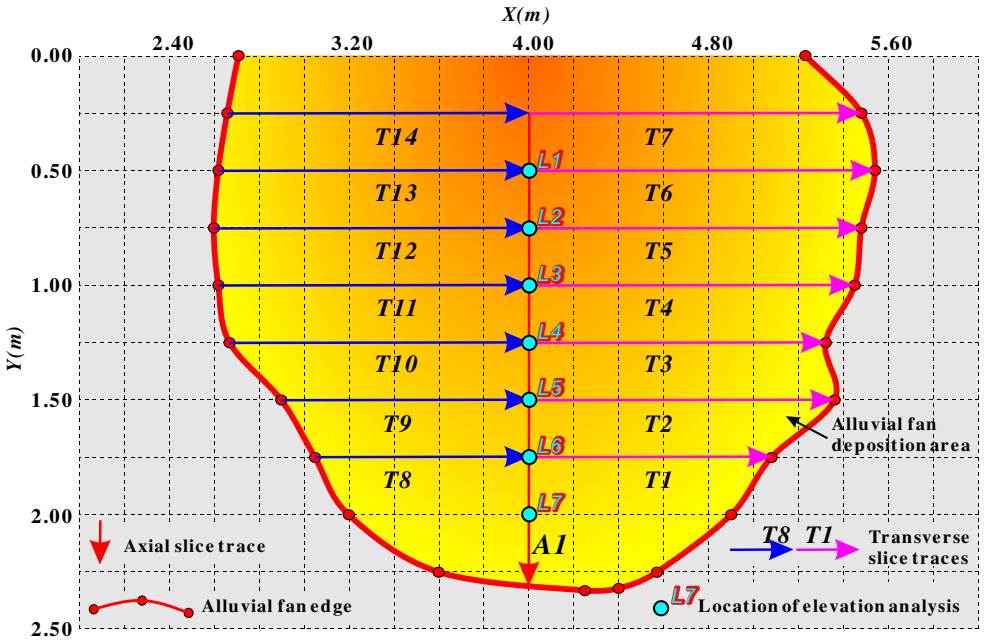

Fig. 4 Coordinate system, location of sliced sections, and elevation measurement points on fan surface

water dispersion and deposition on fan surface, a flood event can be divided into three phases, including (1) the sheet flooding-dominated phase, (2) the unconfined channel-dominated phase, and (3) the confined channel-dominated phase.

According to phase identification in all the 12 flood events, the above three phases occurred in each flood event, sequentially. Records of the fifth flood event were selected as a typical example to analyze the evolution of water dispersion and deposition during a flood event.

The sheet flooding-dominated phase

The sheet flooding-dominated phase is characterize by a large-scale sheet flooding lobe on fan surfaces. At the beginning of a flood event, there was no water on fan surface. Therefore, the water flow first distributed at the lower part of the fan surface (Fig. 5a). As the fast increase of water discharge, the water-covered area expended rapidly (Figs. 2 and 5a). In this phase, the sheet flooding water could cover up to 70% of the fan surface (Fig. 5b, c). The large-scale sheet flooding was driven by high water discharge and resulted in the deposition of a large amount of sediments. The development degree of sheet flooding increased with the discharge growth. Once the discharge reached its peak, the scale of sheet flooding started to wane. A number of radial channels developed on the area that was not covered by sheet flood. All the radial channels were unconfined. As the rapid sedimentation at the lower part of the fan surface, the accommodation space distribution tended to be balanced, and as a result, the development degree of unconfined channels was continuously increased. According to the quantified measurement, the sheet flooding lobe could cover more than 70% of the fan surface when the discharge reached its peak (Fig. 5c). Driven by the high water and sediment supply, the main deposition formed in this phase.

The unconfined channel-dominated phase

The unconfined channel-dominated phase is characterized by frequent and rapid migration of unconfined channels on fan surface. Several radial unconfined channels developed at the fan surface (Fig. 5d, e). According to the quantified measurement, the sheet flooding lobe could only cover up to about 20% area of the fan surface. A typical feature of these unconfined channels is the frequent avulsion at the upper fan and the rapid migration at the lower fan (Fig. 5d, e). In this phase, unconfined channels were fed by a relatively lower discharge than that in the initial phase. As a result, the sedimentation on fan surface was less than that in the initial phase.

The confined channel-dominated phase

The latest phase was dominated by confined channels. Constrained by the limited and continuously decreased water discharge, the sheet flooding lobe did not occur any more (Fig. 5f). Meanwhile, the development degree of channels also decreased. The small-scale channels were confined within the valley formed in the second phase. Limited by the low ability of sediment transportation with a low flow intensity, a very limited amount of sediments was transported to the fan surface. Therefore, the increment of sedimentation in this phase is

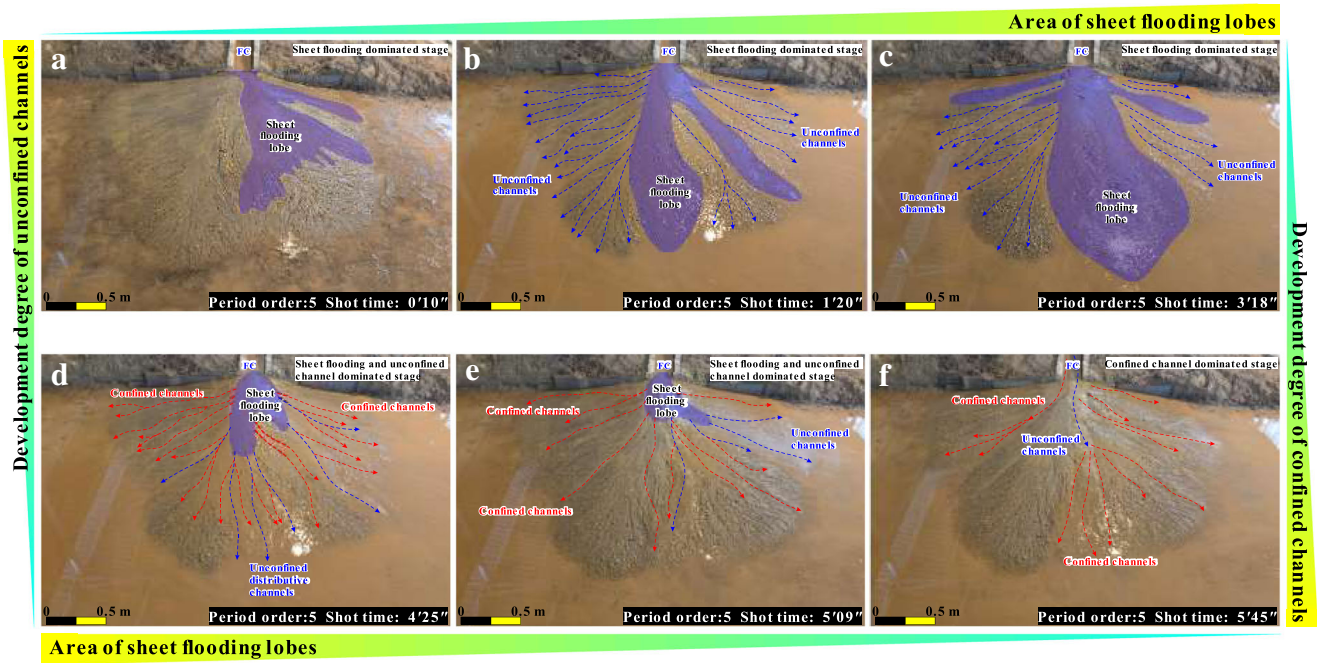

Fig. 5 Evolution of the sedimentary characteristics in the fifth flood event. **a**-**c**. Sheet flooding dominated stage; **d**-**e**. Sheet flooding and unconfined channel dominated stage; **f**. Confined channel dominated stage

significantly lower than that in the above two phases (Fig. 5f), even though the latest phase usually lasts a relatively longer period than the above two phases.

We identified three phases in different flood events and inferred that transition of phases in a single flood event was driven by the variation of the discharge. To check the hypothesis, the relationship between the percentage of fan area covered by flow and water discharge was presented in Fig. 6. We observed and calculated the percentage of fan area covered by flow per half a minute. As a flood event lasted for 6 min, 12 values of the percentage were obtained for each flood event. At the beginning of the fifth flood event, the percentage of fan area covered by flow fast increased with the increase of water discharge (Fig. 6). Once water discharge reached its peak, both the following water discharge and the percentage of fan area covered by flow started to reduced continuously (Fig. 6).

Evolution of the experimental alluvial fan

Flood event-dominated alluvial fan is an important kind of fans which developed in arid to semi-arid climate. A flood event can be regarded as an elementary process to form a large-scale alluvial fan. In other words, this kind of alluvial fan is a complex of sedimentary bodies driven by a number of flood events. In this experiment, 12 flood events were simulated to reproduce the development of a flood event-dominated alluvial fan.

As the sediment bedform was fixed, the accommodation space in the experimental environment is continuously consumed by the deposited sediments. Therefore, the experimental fan would be affected by the decreasing of accommodation space. The spontaneous evolution of the fan was driven by the variation of accommodation space in nature.

We identified three phases in different flood events and recognized that transition of phases in a single flood event was driven by the variation of the discharge (Fig. 6). According to the observation and analysis on the sedimentary process of the 12 flood events, we further inferred that the dominant phase in different flood events was different. From the beginning to the end of the experiment, the sheet flooding deposition continuously decreased; on the contrary, channelized deposition continuously increased. Based on the difference on dominant phase during a flood event, the development of the experimental fan can be divided into three stages including the sheet flooding-dominated stage (Fig. 7(A1–A3)), the unconfined channels dominated stage (Fig. 7(A4–A7)) and the confined channels dominated stage (Fig. 7(A8–A12)).

Sheet flooding-dominated stage

The sheet flooding-dominated stage was the first stage that in which the major sedimentation of the experimental fan formed. As observed by Clarke et al. (2010), there are more than 50% area of the fan surface covered by sheet flood in this stage. During the first four flood events in our experiment, the average percentage of fan surface covered by sheet flood was larger than 50%. According to the recognition of sedimentary phases during the whole sedimentary process of the experimental fan, the fan surface was dominated by sheet flood from the first to the third flood events (Fig. 7(A1–A3)). In this stage, sedimentation mainly appeared near the outlet of the feeder channel.

At this stage, although the water flow rate is very high, the water depth is shallow, the water carries more sediment, and the deposition rate is faster. Therefore, the water flow generally does not erode the deposited sediments (Fig. 8). Dominated by large-area sheet flood, a number of sheet flooding lobes formed and stacked vertically. The sheet flooding lobes are the basic elements to construct the bottom set of the experimental fan (Fig. 8). In addition, fan area increased very fast because of the rapid deposition at the margin of the experimental fan (Fig. 7(A1–A4)). This stage lasted from the first flood event to the fourth flood event.

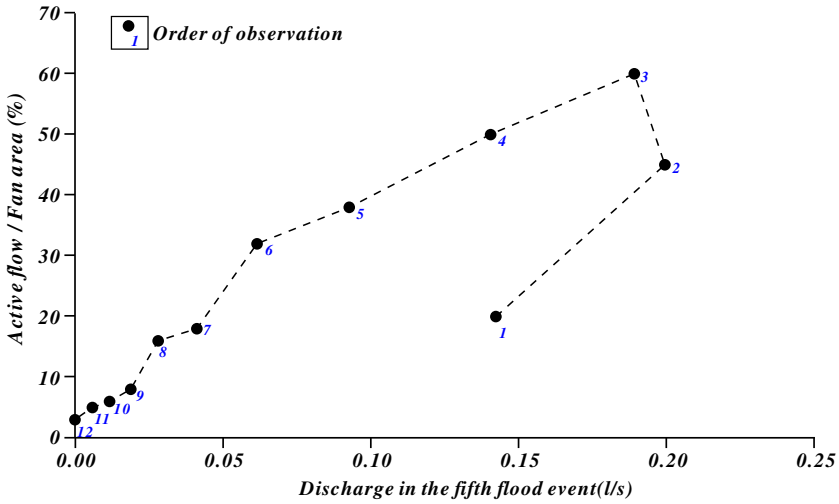

Fig. 6 Relation between discharge and the ratio of active flow to fan surface area. The ratio of active to fan surface area was observed and calculated every half a minute during the fifth flood event

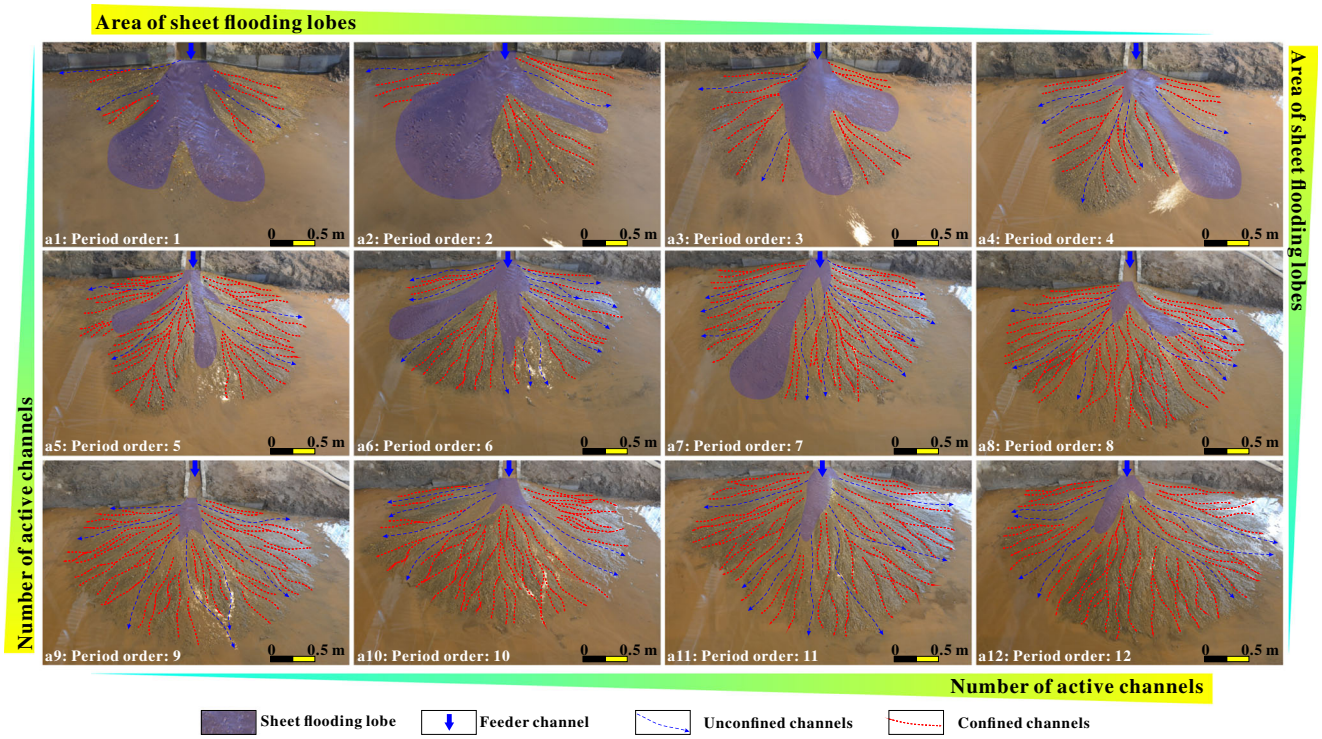

Fig. 7 Geomorphology of the experimental fan at the end of each flood event

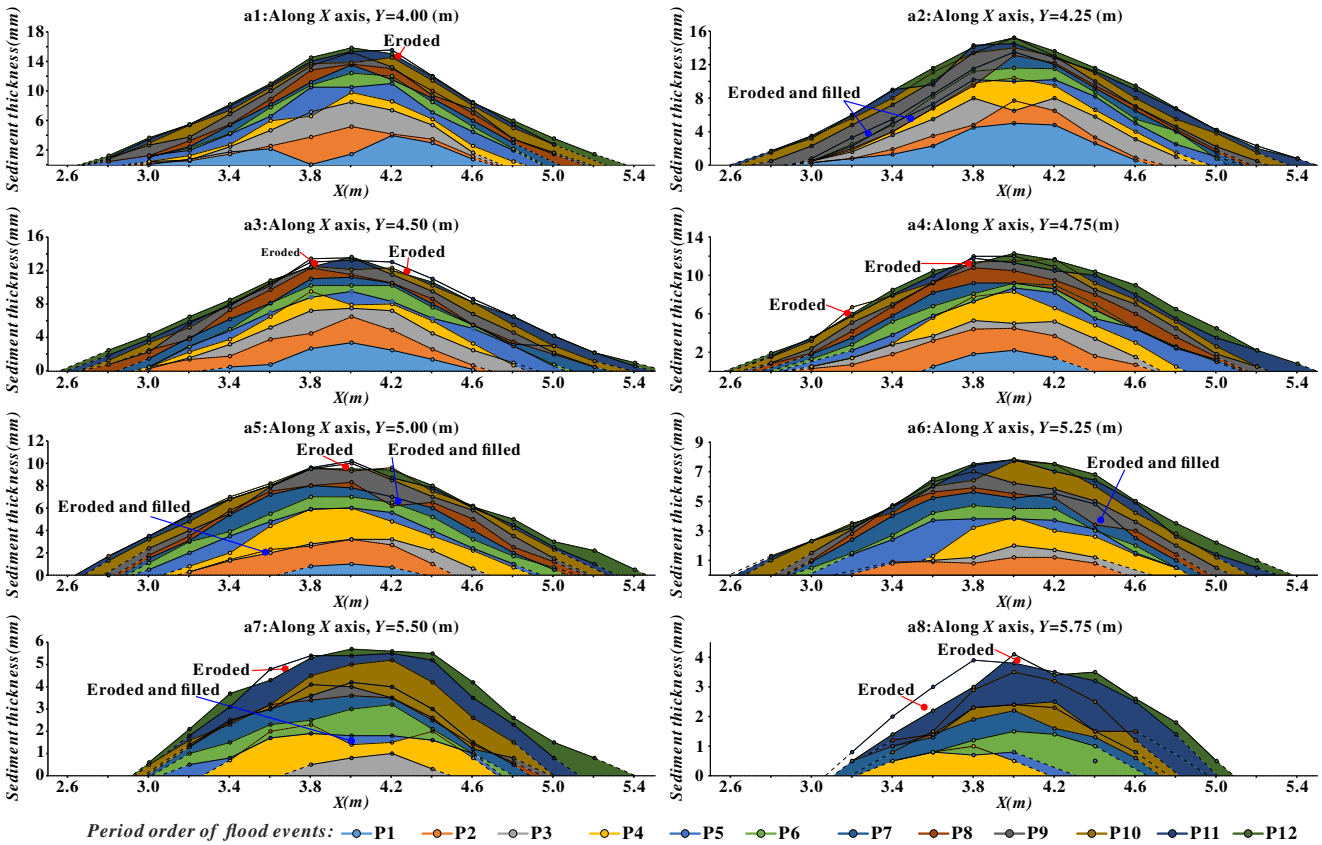

Fig. 8 Eight transverse elevation sections across the experimental fan. Each color represents the sedimentation during a flood event

According to the measurement, the average sediment thickness per one flood event is 4 mm. It is significantly larger than that in the following flood events (Fig. 8).

Unconfined channel-dominated stage

At this stage, even though the water and sediment supply was the same as the sheet flooding-dominated stage, the development degree of sheet flood lobes was significantly lower. In contrast, unconfined channels became the dominant factor to control the sedimentation process (Fig. 7(A5–A7)). According to the measurement, unconfined channels covered up to 60% of the fan surface. Meanwhile, confined channels developed as the branches of the unconfined channels. The channels nearly covered the whole fan surface besides the small-scale sheet flooding lobe (Fig. 7(A5–A7)). Compared to the sheet flooding-dominated stage, the increment of fan area was significantly lower (Fig. 7). In addition, unconfined channels distributed at the lower part of the fan surface, and the confined channels distributed at the relatively higher area (Fig. 7(A6)). Unconfined channels originated from the edge of the sheet flooding lobes, while confined channels originated from the unconfined channels (Fig. 7(A5–A7)).

Confined channel-dominated stage

At the last stage, the development degree of sheet flooding lobes further reduced and only appeared in the flood peak period (Fig. 7(A8–A12)). This stage was characterized by a channel network consisting of a limit number of unconfined channels and a large amount of confined channels. Channels migrated rapidly on fan surface because of the lower slope and less accommodation space (Fig. 9). Four digital images were randomly selected and analyzed to clarify the distribution of channels in different time (Fig. 9a1–a4). The confined channels can be divided into two sets. One is the small-scale confined channels, which widely distributed at the higher area of the fan surface (Fig. 9b). While the other one is the relatively large-scale confined channels, which distributed at the lower area. We recognized the large-scale channels and their middle channel lines were traced and stacked in Fig. 9c. It is obvious that the channels migrated frequently and rapidly. In addition, the migrating confined channels nearly covered all the fan area (Fig. 9c).

Unlike the first two stages, the confined channels that developed during this stage eroded the bottom sediments and caused the sediment to be transported and balanced again. As a result, the average sediment thickness per one flood event was about 1.5 mm (Fig. 8). Therefore, in this stage, sedimentation on fan surface is very balanced.

As observed in the experiment, the evolution from sheet flood to confined channels is probably controlled by the increase of the fan area, and the growth of fan area might have played an important role on the flow patterns. To check the hypothesis, we presented fan area and the percentage of fan area covered by flow in each flood event (Fig. 10). Fan area was measured at the end of each flood event, and the percentage of fan area covered by flow was observed and calculated per half a minute for each flood event. As a flood event lasted for 6 min, 12 values of the percentage were obtained for each flood event. It is shown that fan area was highly related to the percentage of fan area covered by flow (Fig. 10). The percentage of fan area covered by flow significantly decreased with the increase of fan area (Fig. 10) and resulted in the transition of flow pattern on fan surface (Fig. 7).

Fan surface morphologies evolution

(1) Evolution of fan morphology

To quantify the analysis of the fan morphology, we created the fan surface through interpolation based on the measured elevation (Fig. 11), and further calculated the area of the fan at the end of each flood event. Fed by 12 flood events, the area of the fan increased from 1.3 to 5.1 m^2 (Figs. 11 and 12). As the amount of sediment supply in each flood event is the same, the well-fitted curve suggested that the area has a positive relation with the sediment flux (Fig. 12). At the end of the first flood event, the edge of the fan is very irregular. With the continuous growth of the fan, the fan edge becomes smoother.

To quantify the variations of fan edge roughness, we calculated the roughness at the end of each flood event using the function proposed by Straub et al. (2015). The function for roughness calculation is as follows:

$$R_{SL} = \sqrt{\frac{1}{N}\sum_{i=1}^{N}\left(\frac{r_i - \bar{r}}{\bar{r}}\right)^2}$$

Where N is the total number of points defining the edge, r_i are the individual distance measurements, and r is the mean distance from basin entrance to the edge for a certain time stamp. Large values of R_{SL} thus indicate strong variability in the distance from the shoreline to basin inlet when normalized by the mean distance (Straub et al. 2015).

The roughness curve presented in Fig. 13 suggests that the fan edge roughness has a significant and cyclical variation during the first six flood events; meanwhile, the variation obviously decreases during the last six flood events. In addition, the fan edge roughness gradually decreases from 0.087 to 0.046 (Fig. 13). We infer that the fan edge roughness will finally become to a low and stable value if more flood events could be performed.

As mentioned before, with the growth of the experimental fan, the sediment distribution became more balanced since the accommodation space was continuously consumed. However, we observed that there were one or several advantage flow traces at the fan surface at the end of each flood event (Fig. 11). In

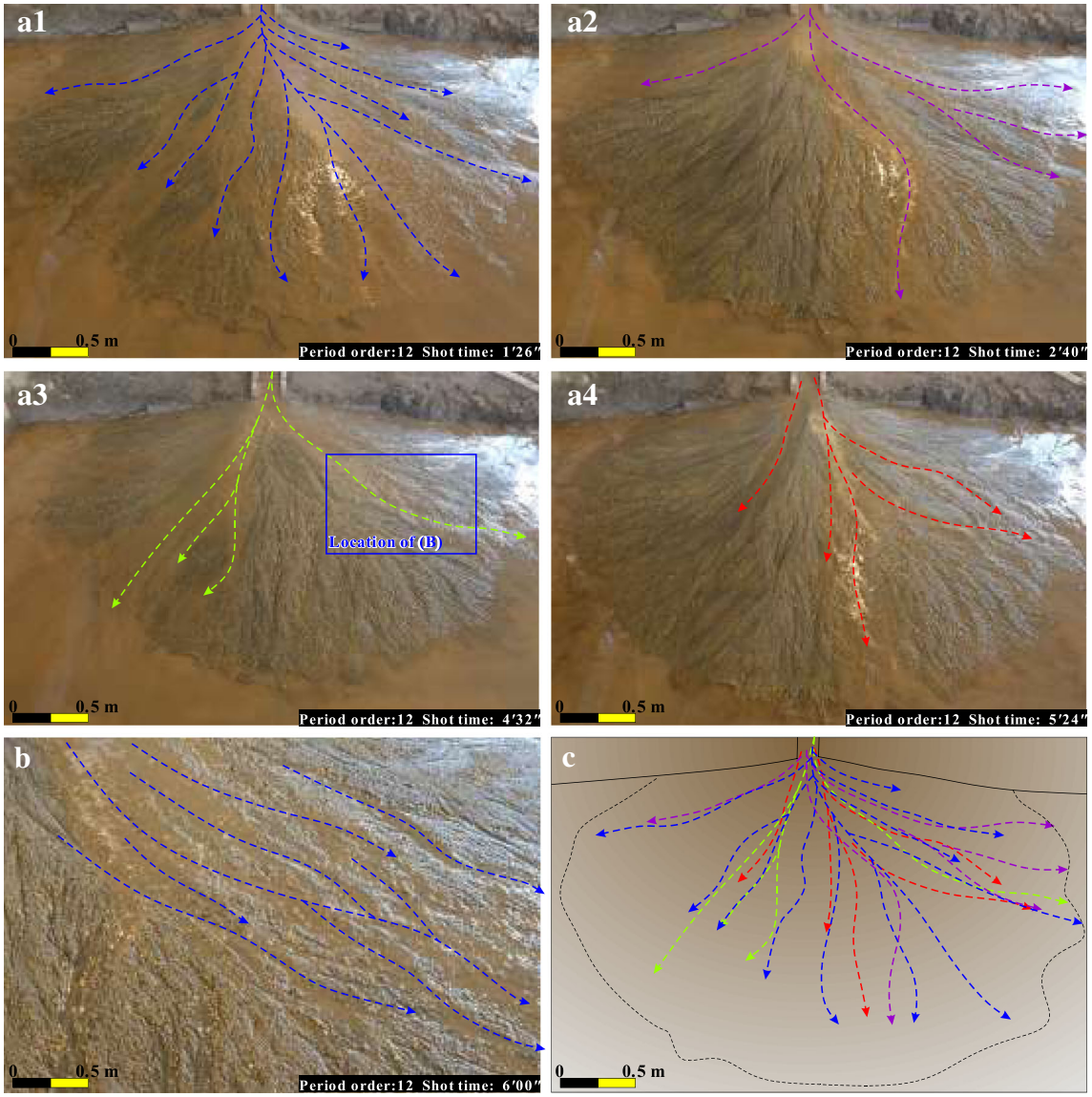

Fig. 9 The migration and evolution of channels on fan surface during the 12th flood event. **a1**–**a4** Distribution of the main channels on fan surface at different time. **b** Distribution of the detailed confined channels within a local area, the location of the picture is presented in **a3**. **c** Stacked channel pathways in **a1**–**a4**

addition, the advantage flow traces located along different directions. Since the advantage flow trace is higher than the other places at the end of a flood event, the flow will "choose" a lower routine and continuously transport and unload sediments along the new flow routine until the accommodation space within the active drainage system was totally occupied. It is worth noting that the amount of advantage flow traces increased with the growth of the experimental fan (Fig. 11).

(2) Vertical aggradation rate

As observed in the experiment, hydrodynamics and sediments unloading laws on fan surface vary from the proximal to distal part. The variations lead to the different vertical aggradation processes. We analyzed the recorded elevation at seven sites which distributed from the proximal to distal part of the experimental fan along the source direction (Figs. 4 and 14).

For the proximal to middle sites (L1–L4), the aggradation rate experiences a fast to medium and finally low process. The conversion process of aggradation rate was roughly correspond to the transition of stages from the sheet flooding-dominated stage to the unconfined channel-dominated stage, and finally the confined channel-dominated stage (Fig. 14).

As for the middle to distal sites (L5–L7), aggradation rate of the experimental fan kept nearly constant (Fig. 14). Therefore, the middle to distal part of the experimental fan are almost not affected by the evolutionary stages of the fan. In addition, we observed that the deposition rate

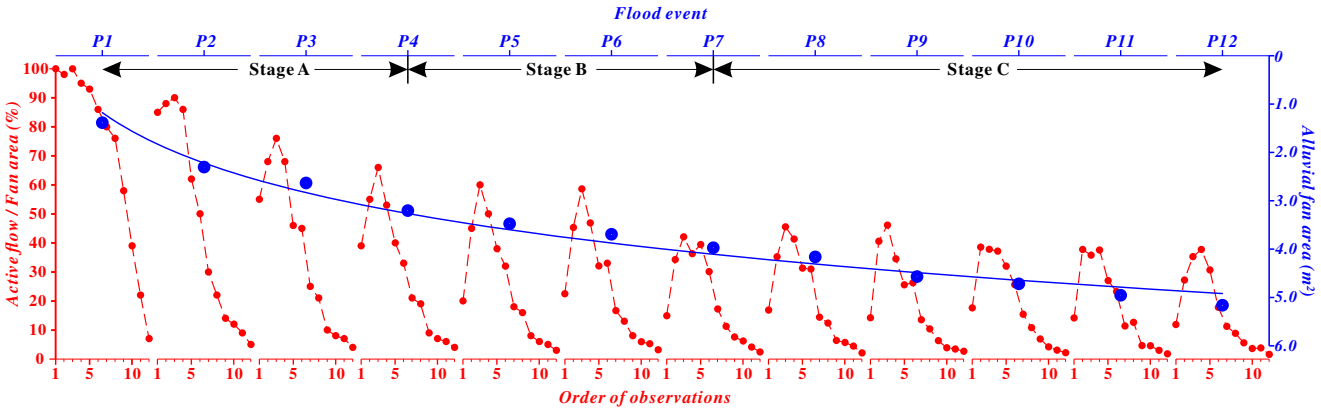

Fig. 10 Relationship between the percentage of fan area covered by flow and fan surface area. Fan surface area was measured at the end of each flood event

decreased from the middle to the distal part of the alluvial fan (Fig. 14).

Internal sedimentary architecture characteristics

Controlled by three different stages, the internal architecture of the experimental fan is supposed to be very complex. To investigate the sedimentary architecture of the flood event-dominated alluvial fan, we constructed 14 transverse sections and a longitudinal section through slicing the alluvial fan based on the experimental results (Figs. 4, 11, and 13). Digital image and the video recorded during the experiment were used as the support information for sedimentary architecture analysis. Observation on slice sections demonstrates that the alluvial fan developed a three-layer structure in vertical direction and shows significantly differences from the proximal part to the distal part (Figs. 15, 16, and 17).

The three-layer structure from the bottom to the top

According to the stage division of the alluvial fan deposition process, a three-layer structure has been recognized on transverse and longitudinal sections. The bottom was mainly formed by sheet floods, the middle layer was mainly constructed by unconfined channels, and the top layer was controlled by confined channels.

The bottom layer formed in the sheet flood-dominated stage, and sediments mainly deposited at the proximal part of the experimental fan (Figs. 15, 16, and 17). A thick and small-area sheet flooding lobe complex formed in this stage. The main architecture element is the sheet flooding lobe. The width of a single lobe is about 0.5 m and the thickness is about 2 mm (Figs. 15 and 16). According to the observations and interpretation on transverse sections, more than four sheet flooding lobes developed during a single flood event (Fig. 16) (A1–A3). Channels are only recognized on the central and upper part of the bottom layer (Fig. 16) (A1–A4). Channel fillings are generally gravels while sheet flooding lobes are generally sand-prone (Fig. 16) (A1–A3).

The middle layer formed in the unconfined channel-dominated stage and associated sedimentation mainly distributed at the middle part of the experimental fan (Fig. 16 (A1–A5)). Compared to the bottom layer, more channel fillings are recognized on transverse sections. Average sediment thickness during a single flood event is about 1 mm (Figs. 15 and 16). It is worth noting that channel fillings extended to the middle part of the experimental fan (Fig. 16 (A2–A4)) and a large fraction of channels was filled by sandy sediments (Fig. 16 (A3–A4)). The main architecture element is channel filling deposits, while the amount and scale of sheet flooding lobes significantly decrease (Fig. 16 (A2–A3)). Sheet flooding lobes generally distributed at the middle to distal part of the experimental fan (Figs. 16 (A3) and 15). Migration and avulsion of the radial unconfined channels formed the balanced sedimentation on the top of the bottom layer. Therefore, sedimentation distribution is more balanced than the bottom layer.

The top layer formed in the confined channel-dominated stage. In this stage, sheet flooding lobes only distributed at the proximal part of the fan surface and its active duration is significantly less than the two previous stages. Therefore, only a few sheet flooding lobes were preserved in the proximal part of experimental fan (Fig. 16(A1)). As we mentioned before, confined channels are the main architecture elements and play a key role on the sedimentary process. Rapidly migrating channels continuously erode the sediments and form new deposits. As a result, only a fraction of channels was preserved and filled with sandy deposits, while the relative higher part formed in the previous stages was eroded (Fig. 16(A2, A6, A7)). Distribution of sediments is more balanced than the two underlying layers (Fig. 16).

Variations of sedimentary architecture characteristics along the longitudinal section

Along the longitudinal section, the three-layer structure and associated sedimentary distribution reveal the complex variations of the sedimentary architecture characteristics (Fig. 17).

Sheet flooding lobes mainly developed within the bottom layer. The thickness of a single sheet flooding lobe decreased from the bottom to the top of the layer (Fig. 17). The bottom layer mainly distributed at the proximal part of the experimental fan, and the thickness of the bottom layer rapidly decreased from 10 to 0 mm within a distance of 1.5 m (Figs. 16 and 17). On the contrary, sedimentation distribution of the middle and top layers is significantly more balanced. Channel fillings preserved in the bottom generally distributed at the upper and proximal part of it (Fig. 17).

In the middle layer, channel fillings extended to the middle part of the experimental fan and the amount of channel fillings also increased (Fig. 17). According to the observation, sediment thickness distribution of the middle and top layers is generally balanced.

In the top layer, scale and preservation of channel fillings obviously decreased. Meanwhile, the erosion of the confined channels is generally reduced than the unconfined channels because the lower hydrodynamics and smaller scale of the confined channels (Fig. 17).

In addition, the preservation of channel fillings decreased from the proximal part to the distal part of the experimental fan.

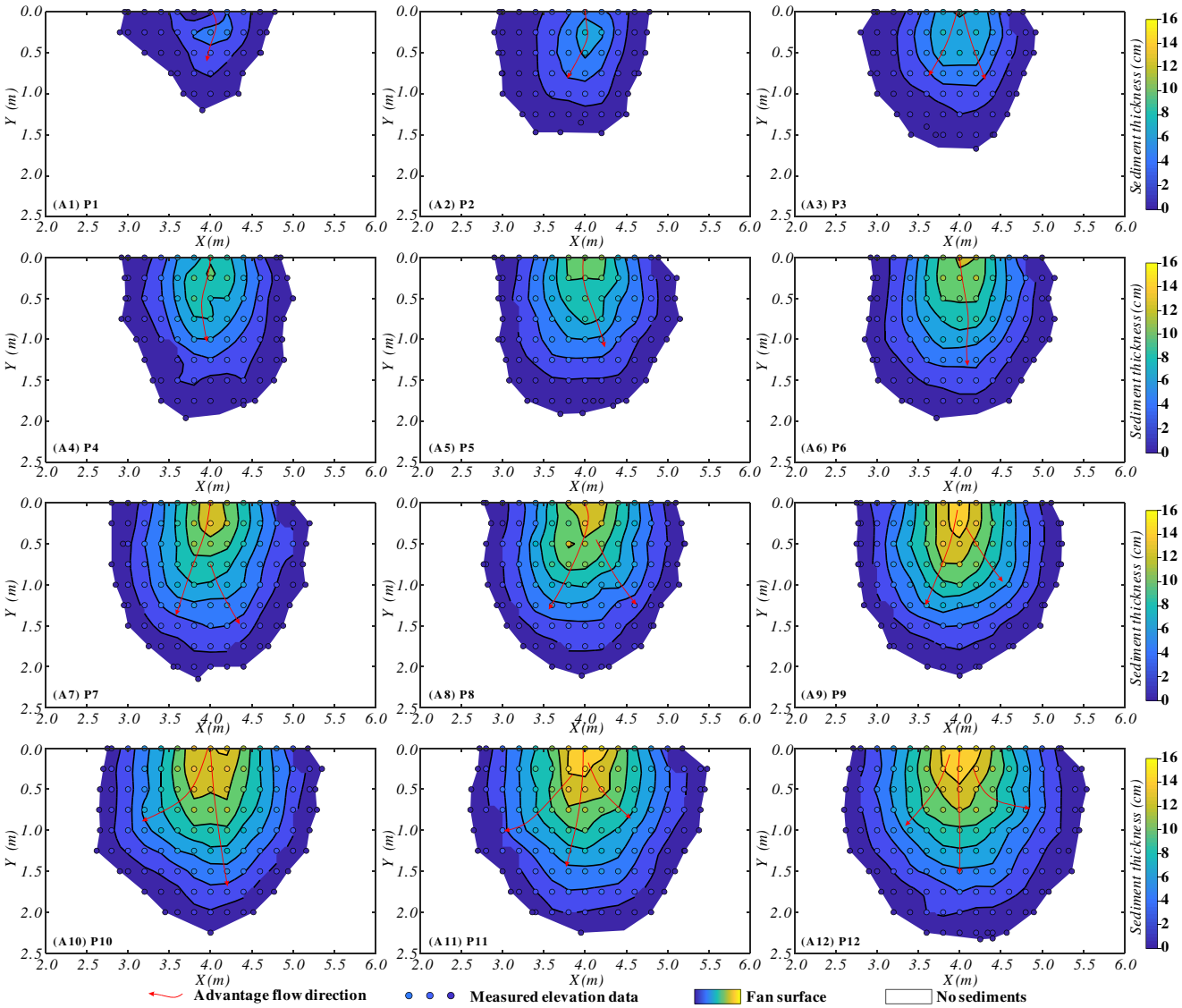

Fig. 11 Geomorphology of the experimental fan at the end of each flood event. The advantage flow trace has been recognized and presented

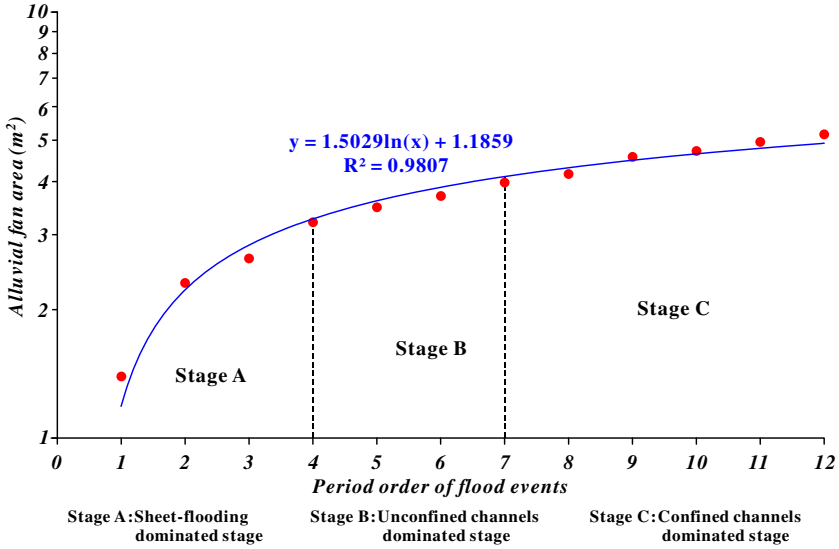

Fig. 12 Variations of the fan area at the end of 12 flood events. A well-fitted curve suggests that the area has a positive relation with the sediment flux. In the function, x is the period order of flood events and y is alluvial fan area

Discussions

Implication for the depositional process during a single flood event

According to the observation on water dispersion and deposition on fan surface, a flood event can be divided into three phases, including (1) the sheet flooding-dominated phase, (2) the unconfined channel-dominated phase, and (3) the confined channel-dominated phase. In a typical flood event, the discharge fast increased to its peak and gradually decrease to zero. With the decrease of discharge, the flow pattern transformed from sheet flooding to unconfined channels and end with confined channels. It is inferred that the discharge from the feeder channel is the dominant factor controlling the flow patterns on fan surface (e.g., Hooke, 1967; Le Hooke and Rohrer, 1979; Van den Berg, 1995; Whipple et al., 1998; Clarke et al., 2010). In addition, the discharge and associated flow pattern determined the sedimentation on fan surface. The main deposition occurred during the first and second phase, while the modification by confined channels on fan surface mainly occurred at the third phase (e.g., Yin et al., 2013; Feng et al., 2017).

Implication for the depositional process of the flood event-dominated alluvial fans

The recorded depositional process of the experimental fan presented many fundamental characteristics of an alluvial fan fed and dominated by flood events, including the sheet flooding process and associated lobes, the occurrence of unconfined channels and confined channels, and the transformation from the unconfined to confined channels. These observed features and associated evolution of alluvial fan in this experiment were consistent with the previous studies on fluvial fans (Van Dijk et al., 2009; Clarke et al., 2010; Clarke, 2015; Delorme et al., 2016, 2018). The experiments performed by Clarke et al. (2010)

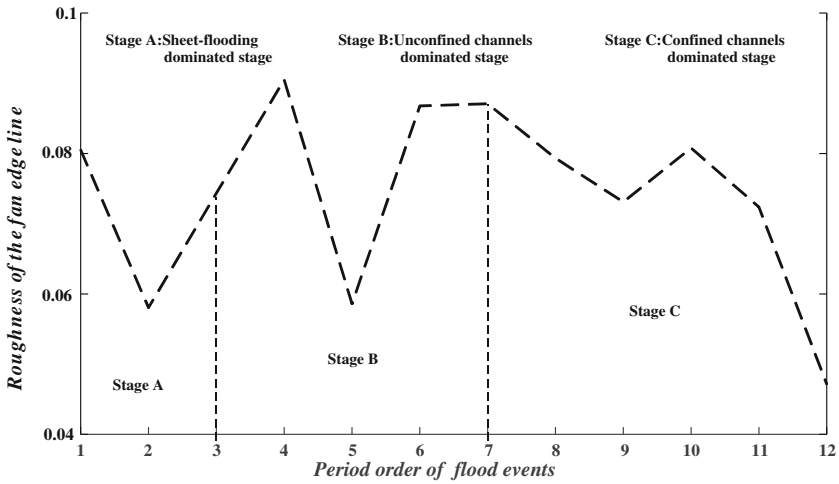

Fig. 13 Variation of the fan edge roughness. The function for fan edge roughness was proposed by Straub et al. (2015)

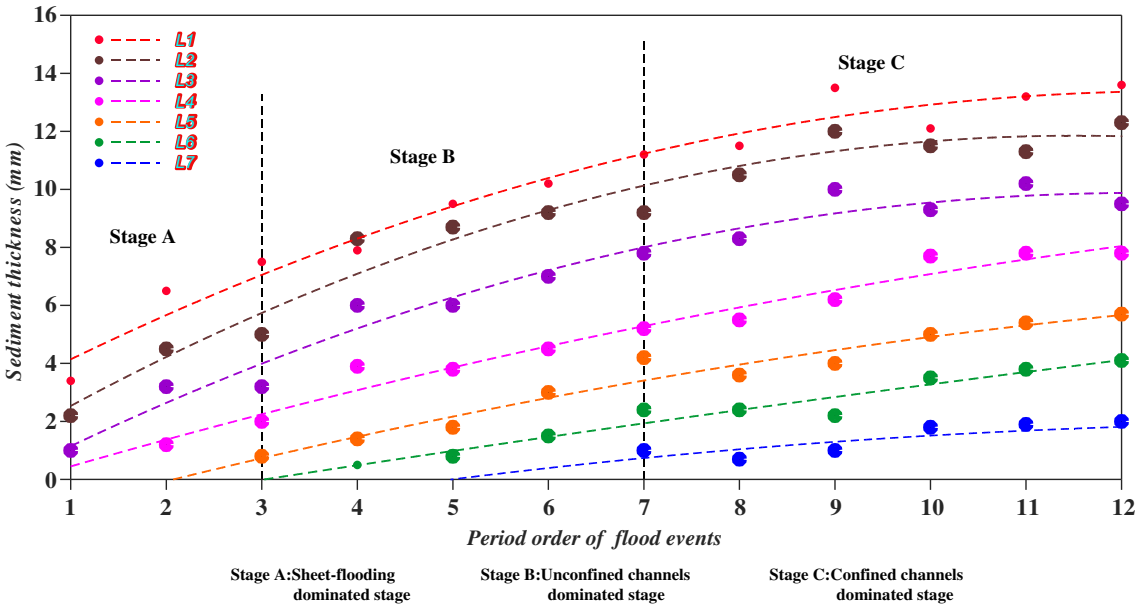

Fig. 14 Sediment thickness variations at a set of sites along the longitudinal section A1 during the experiment

suggested that the alluvial fan fed by constant water and sediment supply experienced three major stages including the sheet flow-dominated-unstable channelized stage, the lateral migration stage, and single channel stage. The flood event-dominated alluvial fan also experienced three stages including sheet flooding-dominated stage, the unconfined channel-dominated stage, and the confined channel-dominated stage. Both the alluvial fans constructed by Clarke et al. (2010) and the experiment presented in this paper were formed without extrinsic conditions. Therefore, the sedimentary process of alluvial fan under constant boundary conditions varied from the beginning to the end, strongly. Similar variations can also be observed in fluvial fan deltas (Van Dijk et al., 2008), alluvial fans (Hamilton et al., 2013), fluvial deltas (Muto and Steel, 2004; Trampush et al., 2017), and fluvial systems (Hajek and Straub, 2017).

Even though the evolution of both the experimental fan simulated with constant water discharge and sediment supply (Clarke et al., 2010) and the flood event-dominated fan experienced three stages, the sedimentation processes of the two fans are quite different. In the experiment presented by Clarke et al. (2010), flow pattern on fan surface was gradually changed. In contrast, the experimental fan dominated by flood

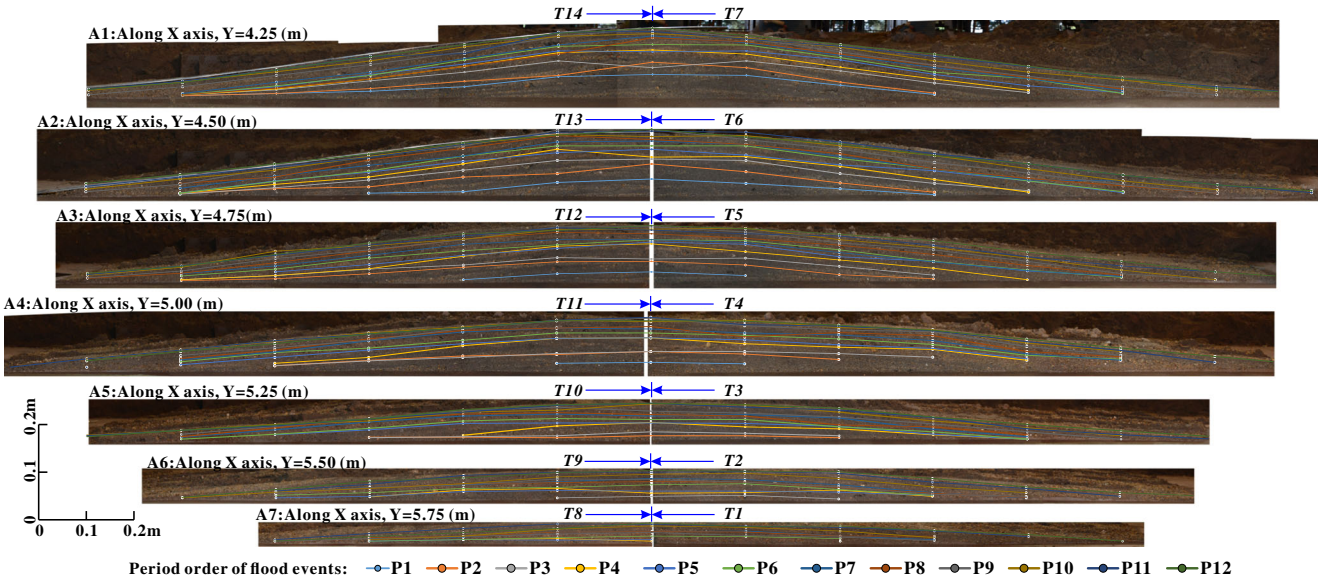

Fig. 15 Pictures of 14 transverse slice sections of the experimental fan. Surface elevation lines at the end of each flood event have been presented on the sections

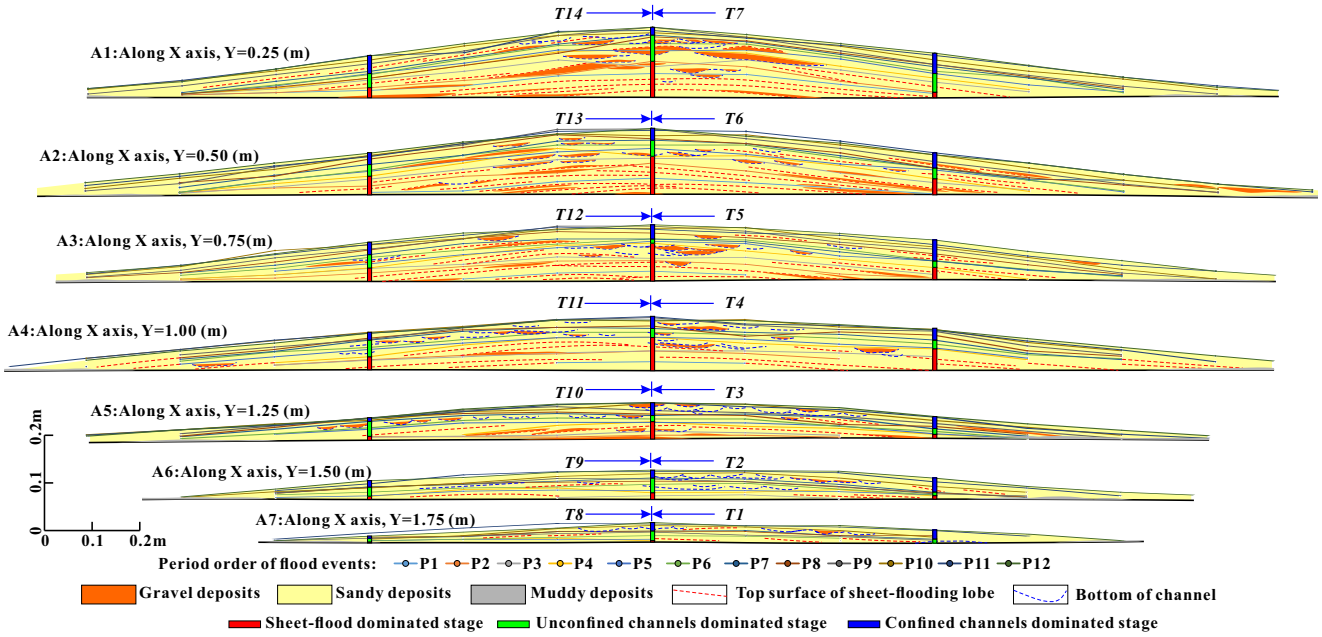

Fig. 16 Sedimentary interpretation of the 14 sections in Fig. 8

events experienced a number of short-time cycle on flow patterns, and the cycles were also varied from the beginning to the end of the experiment.

Using the measured elevation data and fan edge location, the evolution of the fan morphology was analyzed. Fed by periodic flood events, fan area increased from 1.3 to 5.1 m^2

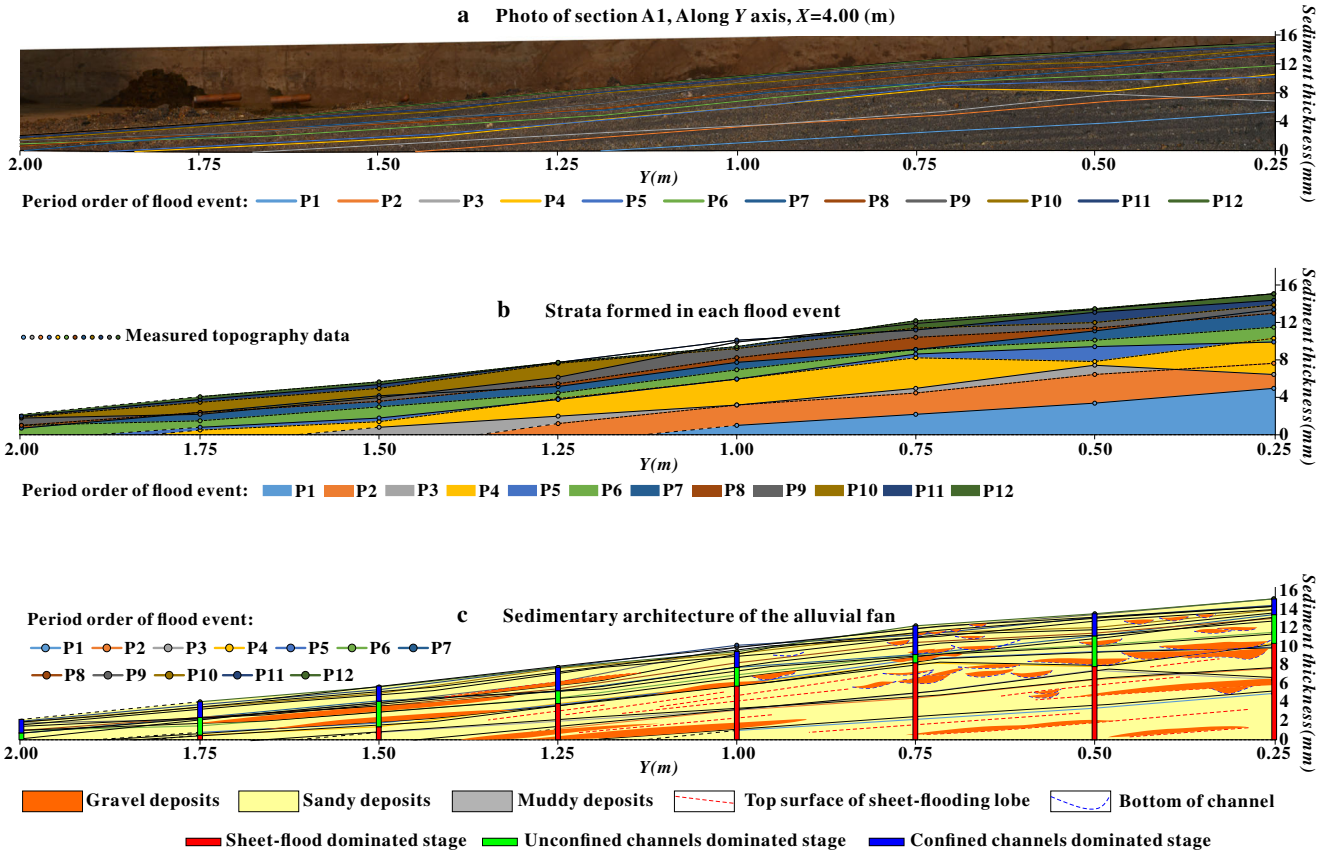

Fig. 17 Picture and interpretation on stratigraphy and sedimentary architecture of the longitudinal section. **a** Digital picture of the longitudinal section. **b** The stratigraphy based on the measured fan surface data. **c** Sedimentary architecture analysis of the longitudinal section

while the roughness of fan edge decreased from 0.87 to 0.046. It is worth noting that a well-fitted curve suggests that the area has a positive relation with the sediment flux and the growth rate of fan area gradually decreases with the continuous sedimentation. Similar variations of sedimentary system area have been observed in a number of experiments (Nicholas et al., 2009; Straub et al., 2015; Clarke et al., 2010, 2015). We infer that with the increment of the area of a sedimentary system, more and more sediments need to be supplied to keep a constant area growth rate.

Local variations in fan slope have been observed by numerous experimental studies (Delorme et al., 2018; Reitz and Jerolmack, 2012; Clarke et al., 2010; Van Dijk et al., 2009) and field works (Blair and Mcpherson, 1992; Blair, 2001; Shukla et al., 2001). And the variations seem to be controlled by internal fan dynamics and the flow position on the fan surface (Clarke, 2015). In our experiment, the growth rate varies with the locations on the experimental fan, too. At the proximal part, the elevation experienced a rapid deposition, a normal deposition, and a slow deposition process. As for the middle to distal part, the experimental fan experienced a single normal deposition process.

The physical experiment provides abundant information of the sedimentary characteristics and evolution of the flood event-dominated alluvial fan. According to the constant boundary conditions, the spontaneous evolution of the fan is only controlled by autogenic factors. The experiment demonstrates that, even though the extrinsic boundary conditions keep constant, the depositional process and associated sedimentary architecture of alluvial fans are still very complex and more attention needs to be paid on the effect of autogenic factors during sedimentation (Hajek and Straub, 2017; Mouchené et al., 2017; Trampush et al., 2017; de Haas et al., 2016; Zhang et al., 2016; Clarke, 2015; Hamilton et al., 2013; Van Dijk et al., 2012, 2009; Clarke et al., 2010; Muto and Steel, 2004).

Insights to the internal sedimentary architecture of the flood event-dominated alluvial fans

We further investigate the sedimentary architecture of the experimental fan which experienced three different stages. A three-layer structure has been presented. The bottom layer was dominated by sheet flooding process and the main preserved architecture element is the sheet flooding lobe. This layer was mainly consisted of sheet flooding lobes. Channel fillings are only recognized on the central and upper part of the bottom layer. The middle layer was formed by frequently migrating unconfined channels. The main architecture element is channel filling deposits, while the amount and scale of sheet flooding lobes significantly decrease. The small-scale sheet flooding lobes generally distributed at the middle to distal part of the experimental fan. Within the top layer, only a few sheet flooding lobes were preserved in the proximal part of experimental fan. Rapidly migrating channels continuously erode the sediments and form new deposits. Thus, only a fraction of channels was preserved and filled with sandy deposits, while the relative higher part formed in the formal stages was eroded. The similar vertical structure has been observed on experimental fans (Reitz and Jerolmack, 2012), outcrops (Blair, 1987; Blair and McPherson, 1994; Fidolini et al., 2013), and subsurface records (Yin et al., 2013) of various types of alluvial fans. The variations of sedimentary architecture were investigated through a longitudinal slice section. Sheet flooding lobes were mainly preserved in the proximal part of the bottom layer whereas the channel fillings were preserved at the distal part of the layer. The middle and top layer consist of unconfined channel fillings and confined channel fillings, respectively. Variations of sedimentary architecture decrease from the proximal part to the distal part (Bull, 1977; Stanistreet and McCarthy, 1993; Sáez et al., 2007; Ventra and Nichols, 2014; Moscariello, 2018).

Conclusions

In order to gain more understanding of the sedimentary process and associated internal architecture of the flood event-driven alluvial fan, a flume experiment is performed in this paper. Aiming at the spontaneously sedimentary process and evolution without the constrain of extrinsic conditions, 12 same flood events are simulated to feed the experimental fan. The relevant evolution pattern of the fan was obtained by an integrated analysis of digital images and the elevation data. Internal architecture of the experimental fan was anatomy through sliced sections. The following conclusions can be derived from the study:

(1) A flood event experienced a high fluidity period and a following low fluidity period. Driven by the variations of hydrodynamics and sediment transportation, a flood event can be subdivided into three phases, including the sheet flooding-dominated phase, the unconfined channel-dominated phase, and the confined channel-dominated phase. The discharge from the feeder channel is the dominant factor controlling the flow patterns on fan surface.
(2) Due to the constant extrinsic condition and the continuously consumption of the limited accommodation space, the experimental fan experienced three different stages including the sheet flooding-dominated stage, the unconfined channel-dominated stage, and the confined channel-dominated stage.
(3) Controlled by the three different stages, a three-layer structure formed in the deposited experimental fan. The bottom layer is a thick and small-area sheet flooding lobe

complex formed in the sheet flood-dominated stage, and sediments mainly deposited at the proximal part of the experimental fan. Compared to the bottom layer, more channel fillings are recognized in the middle layer. The main architecture element is channel filling deposits, while the amount and scale of sheet flooding lobes significantly decreased. Confined channels are the main architecture elements preserved in the top layer. Rapidly migrating confined channels continuously erode the sediments and form new deposits.

(4) Local variations in fan aggradation have been measured and analyzed. At the proximal part, the elevation experienced a rapid deposition, a normal deposition, and a slow deposition process. As for the middle to distal part, the experimental fan experienced a single normal deposition process. Fan area is positive related to the sediment flux while its growth rate decreases with the increment of it. The roughness of fan edge changed rapidly in sheet flooding dominated and unconfined channel-dominated stages, and gradually decreased in confined channel-dominated stage.

(5) The experimental fan is an ideal simulation of the flood event-dominated fan in natural systems. The sedimentary process and associated evolution are similar to the natural fans and can be used for predicting the development of active natural fans. The internal sedimentary architecture can be regarded as a frame for architecture analysis on subsurface oil and gas reservoir which formed by flood event-dominated fans.

Acknowledgments We would like to express our gratitude to Prof Zhongbao Liu and Mr. Qinyu Xia, who offered many helpful concerns to this study. Special thanks go to journal editor and reviewers for the insightful suggestions to improve the manuscript.

Funding This study was financially supported by the National Natural Science Foundation of China (Nos. 41802123 and 41502126), China Postdoctoral Science Foundation funded project (No. 2018M630843), and National Science and Technology Major Project of China (No. 2016ZX05027-002-007). We dedicate this work to them for their financial support.

References

Al-Sarawi AM (1988) Morphology and facies of alluvial fans in Kadhmah Bay, Kuwait. J Sediment Res 58(5):902–907

Bahrami S (2013) Tectonic controls on the morphometry of alluvial fans around Danehkhoshk anticline, Zagros, Iran. Geomorphology 180: 217–230

Blair TC (1987) Tectonic and hydrologic controls on cyclic alluvial fan, fluvial, and lacustrine rift-basin sedimentation, Jurassic-Lowermost Cretaceous Todos Santos Formation, Chiapas, Mexico. J Sediment Res 57(5):845–862

Blair TC (1999a) Cause of dominance by sheetflood vs. debris-flow processes on two adjoining alluvial fans, Death Valley, California. Sedimentology 46(6):1015–1028

Blair TC (1999b) Alluvial fan and catchment initiation by rock avalanching, Owens Valley, California. Geomorphology 28(3–4):201–221

Blair TC (2000) Sedimentology and progressive tectonic unconformities of the sheetflood-dominated Hell's Gate alluvial fan, Death Valley, California. Sediment Geol 132(3–4):233–262

Blair TC (2001) Outburst flood sedimentation on the proglacial Tuttle Canyon alluvial fan, Owens Valley, California, USA. J Sediment Res 71(5):657–679

Blair TC, McPherson JG (1992) The Trollheim alluvial fan and facies model revisited. Geological Society of America Bulletin, 104(6): 762–769

Blair TC, McPherson JG (1994) Alluvial fans and their natural distinction from rivers based on morphology, hydraulic processes, sedimentary processes, and facies assemblages. J Sediment Res 64(3a):450–489

Brierley GJ, Liu K, Crook KA (1993) Sedimentology of coarse-grained alluvial fans in the Markham Valley, Papua New Guinea. Sediment Geol 86(3–4):297–324

Bull WB (1977) The alluvial-fan environment. Prog Phys Geogr 1(2): 222–270

Chakraborty PP, Paul P (2014) Depositional character of a dry-climate alluvial fan system from Palaeoproterozoic rift setting using facies architecture and palaeohydraulics: example from the Par Formation, Gwalior Group, central India. J Asian Earth Sci 91:298–315

Chen LQ, Guo FS (2017) Upper cretaceous alluvial fan deposits in the Jianglangshan Geopark of Southeast China: implications for bedrock control on Danxia landform evolution. J Mt Sci 14(5):926–935

Clarke LE (2015) Experimental alluvial fans: advances in understanding of fan dynamics and processes. Geomorphology 244:135–145

Clarke L, Quine TA, Nicholas A (2010) An experimental investigation of autogenic behaviour during alluvial fan evolution. Geomorphology 115(3–4):278–285

Davidson SK, Hartley AJ, Weissmann GS, Nichols GJ, Scuderi LA (2013) Geomorphic elements on modern distributive fluvial systems. Geomorphology 180:82–95

de Gibert JM, Sáez A (2009) Paleohydrological significance of trace fossil distribution in Oligocene fluvial-fan-to-lacustrine systems of the Ebro Basin, Spain. Palaeogeogr Palaeoclimatol Palaeoecol 272(3–4):162–175

de Haas T, van den Berg W, Braat L, Kleinhans MG (2016) Autogenic avulsion, channelization and backfilling dynamics of debris-flow fans. Sedimentology 63(6):1596–1619

DeCelles PG, Gray MB, Ridgway KD, Cole RB, Pivnik DA, Pequera N, Srivastava P (1991) Controls on synorogenic alluvial-fan architecture, Beartooth Conglomerate (Palaeocene), Wyoming and Montana. Sedimentology 38(4):567–590

Delorme P, Voller V, Paola C, Devauchelle O, Lajeunesse É, Barrier L, Métivier F (2016) Self-similar growth of a bimodal laboratory fan. Earth Surface Dynamics 5(2):239–252

Delorme P, Devauchelle O, Barrier L, Métivier F (2018) Growth and shape of a laboratory alluvial fan. Phys Rev E 98(1):012907

Ettinger S, Manville V, Kruse S, Paris R (2014) GPR-derived architecture of a lahar-generated fan at Cotopaxi volcano, Ecuador. Geomorphology 213:225–239

Feng, W. J., Wu, S. H., Yin, S. L., Zhang, L., Li, J. F., & Xia, Q. Y. 2017. Internal architecture characteristics of Triassic arid alluvial fan in northwestern margin of Junggar basin. Geological Review

Fidolini F, Ghinassi M, Aldinucci M, Billi P, Boaga J, Deiana R, Brivio L (2013) Fault-sourced alluvial fans and their interaction with axial fluvial drainage: an example from the Plio-Pleistocene Upper Valdarno Basin (Tuscany, Italy). Sediment Geol 289:19–39

Fontana A, Mozzi P, Marchetti M (2014) Alluvial fans and megafans along the southern side of the Alps. Sediment Geol 301:150–171

Galve JP, Alvarado GE, Pérez-Peña JV, Mora MM, Booth-Rea G, Azañón JM (2016) Megafan formation driven by explosive volcanism and active tectonic processes in a humid tropical environment. Terra Nova 28(6):427–433

Goswami PK (2017) Depositional processes in the distal part of a large alluvial fan's feeder channel in Himalayan foothills, India. Geol J 52(5):733–744

Guerit L, Métivier F, Devauchelle O, Lajeunesse E, Barrier L (2014) Laboratory alluvial fans in one dimension. Phys Rev E 90(2): 022203

Hajek EA, Straub KM (2017) Autogenic sedimentation in clastic stratigraphy. Annu Rev Earth Planet Sci 45:681–709

Hamilton PB, Strom K, Hoyal DC (2013) Autogenic incision-backfilling cycles and lobe formation during the growth of alluvial fans with supercritical distributaries. Sedimentology 60(6):1498–1525

Heward AP (1978) Alluvial fan and lacustrine sediments from the Stephanian A and B (La Magdalena, Cinera—Matallana and Sabero) coalfields, northern Spain. Sedimentology 25(4):451–488

Hooke RL (1967) Processes on arid-region alluvial fans. The Journal of Geology 75(4):438–460

Ielpi A, Ghinassi M (2016) A sedimentary model for early Palaeozoic fluvial fans, Alderney Sandstone Formation (Channel Islands, UK). Sediment Geol 342:31–46

Latrubesse EM (2015) Large rivers, megafans and other Quaternary avulsive fluvial systems: a potential "who's who" in the geological record. Earth Sci Rev 146:1–30

Le Hooke RB, Rohrer WL (1979) Geometry of alluvial fans: effect of discharge and sediment size. Earth Surface Processes 4(2):147–166

Lin C, Liu S, Zhuang Q, Steel RJ (2018) Sedimentation of Jurassic fan-delta wedges in the Xiahuayuan basin reflecting thrust-fault movements of the western Yanshan fold-and-thrust belt, China. Sediment Geol 368:24–43

López-Gamundí OR, Astini RA (2004) Alluvial fan–lacustrine association in the fault tip end of a half-graben, northern Triassic Cuyo basin, western Argentina. J S Am Earth Sci 17(4):253–265

Lu C, Liu Z, Jia H, Dai Q, Li M, Ren M, Xia S, Li L, Wang S (2018) The controls of geomorphology and sediment supply on sequence stratigraphic architecture and sediment partitioning of the lacustrine rift basin in the Es_3 of Liuzan area, Nanpu Sag, Bohai Bay Basin, China. Aust J Earth Sci 65(2):275–301

Majumder D, Ghosh P (2018) Characteristics of the drainage network of the Kosi Megafan, India and its interaction with the August 2008 flood flow. Geol Soc Lond, Spec Publ 440(1):307–326

Moscariello A (2018) Alluvial fans and fluvial fans at the margins of continental sedimentary basins: geomorphic and sedimentological distinction for geo-energy exploration and development. Geol Soc Lond, Spec Publ 440(1):215–243

Mouchené M, van der Beek P, Carretier S, Mouthereau F (2017) Autogenic versus allogenic controls on the evolution of a coupled fluvial megafan–mountainous catchment system: numerical modelling and comparison with the Lannemezan megafan system (northern Pyrenees, France). Earth Surface Dynamics 5(1):125–143

Muravchik M, Bilmes A, D'Elia L, Franzese JR (2014) Alluvial fan deposition along a rift depocentre border from the Neuquén Basin, Argentina. Sediment Geol 301:70–89

Muto T, Steel RJ (2004) Autogenic response of fluvial deltas to steady sea-level fall: implications from flume-tank experiments. Geology 32(5):401–404

National Research Council. 1996. Alluvial fan flooding. National Academies Press

Nichols G (2018) High-resolution estimates of rates of depositional processes from an alluvial fan succession in the Miocene of the Ebro Basin, northern Spain. Geol Soc Lond, Spec Publ 440(1):159–173

Nicholas AP, Clarke L, Quine TA (2009) A numerical modelling and experimental study of flow width dynamics on alluvial fans. Earth Surface Processes and Landforms, 34(15):1985–1993

Nilsen, T. H. 1982. Alluvial fan deposits, in Scholle, P. A., and Spearing, D., eds., Sandstone depositional environments: American Association of Petroleum Geologists Memoir. 31, 49–86

Ramos E, Busquets P, Vergés J (2002) Interplay between longitudinal fluvial and transverse alluvial fan systems and growing thrusts in a piggyback basin (SE Pyrenees). Sediment Geol 146(1–2):105–131

Reitz MD, Jerolmack DJ (2012) Experimental alluvial fan evolution: channel dynamics, slope controls, and shoreline growth. J Geophys Res Earth Surf 117(F2)

Ridgway KD, Decelles PG (1993) Stream-dominated alluvial fan and lacustrine depositional systems in Cenozoic strike-slip basins, Denali fault system, Yukon Territory, Canada. Sedimentology 40(4):645–666

Sáez A, Anadón P, Herrero MJ, Moscariello A (2007) Variable style of transition between Palaeogene fluvial fan and lacustrine systems, southern Pyrenean foreland, NE Spain. Sedimentology 54(2):367–390

Sahu S, Saha D, Dayal S (2015) Sone megafan: a non-Himalayan megafan of craton origin on the southern margin of the middle Ganga Basin, India. Geomorphology 250:349–369

Shukla UK, Singh IB, Sharma M, Sharma S (2001) A model of alluvial megafan sedimentation: Ganga Megafan. Sediment Geol 144(3–4): 243–262

Singh H, Parkash B, Gohain K (1993) Facies analysis of the Kosi megafan deposits. Sediment Geol 85(1–4):87–113

Sorriso-Valvo M, Antronico L, Le Pera E (1998) Controls on modern fan morphology in Calabria, Southern Italy. Geomorphology 24(2–3): 169–187

Stanistreet IG, McCarthy TS (1993) The Okavango Fan and the classification of subaerial fan systems. Sediment Geol 85(1–4):115–133

Straub KM, Esposito CR (2013) Influence of water and sediment supply on the stratigraphic record of alluvial fans and deltas: process controls on stratigraphic completeness. J Geophys Res Earth Surf 118(2):625–637

Straub KM, Wang Y (2013) Influence of water and sediment supply on the long-term evolution of alluvial fans and deltas: statistical characterization of basin-filling sedimentation patterns. J Geophys Res Earth Surf 118(3):1602–1616

Straub KM, Li Q, Benson WM (2015) Influence of sediment cohesion on deltaic shoreline dynamics and bulk sediment retention: a laboratory study. Geophysical Research Letters, 42(22):9808–9815

Trampush SM, Hajek EA, Straub KM, Chamberlin EP (2017) Identifying autogenic sedimentation in fluvial-deltaic stratigraphy: evaluating the effect of outcrop-quality data on the compensation statistic. J Geophys Res Earth Surf 122(1):91–113

Trendell AM, Atchley SC, Nordt LC (2013) Facies analysis of a probable large-fluvial-fan depositional system: the upper Triassic Chinle formation at petrified forest national park, Arizona, U.S.A. J Sediment Res 83(10):873–895

Van den Berg JH (1995) Prediction of alluvial channel pattern of perennial rivers. Geomorphology 12(4):259–279

van der Meulen S (1986) Eocene sheetflood systems and transitional fan-deltas, Southern Pyrenees, Spain. Geol J 21(2):169–199

Van Dijk, M., Postma, G., Kleinhans, M. G., Dohmen-Janssen, C. M., & Hulchser, S. J. M. H. 2008. Autogenic cycles of sheet and channelised flow on fluvial fan-deltas. River, coastal, and estuarine morphodynamics: London, Taylor and Francis Group, 823–828

Van Dijk M, Postma G, Kleinhans MG (2009) Autocyclic behaviour of fan deltas: an analogue experimental study. Sedimentology 56(5): 1569–1589

Van Dijk M, Kleinhans MG, Postma G et al (2012) Contrasting morphodynamics in alluvial fans and fan deltas: effect of the downstream boundary[J]. Sedimentology, 59(7):2125–2145

Ventra D, Nichols GJ (2014) Autogenic dynamics of alluvial fans in endorheic basins: outcrop examples and stratigraphic significance. Sedimentology 61(3):767–791

Wang J, Jiang Z, Zhang Y, Gao L, Wei X, Zhang W, Liang Y, Zhang H (2015) Flume tank study of surface morphology and stratigraphy of a fan delta. Terra Nova 27(1):42–53

Weissmann GS, Mount JF, Fogg GE (2002) Glacially driven cycles in accumulation space and sequence stratigraphy of a stream-dominated alluvial fan, San Joaquin Valley, California, USA. J Sediment Res 72(2):240–251

Whipple KX, Parker G, Paola C, Mohrig D (1998) Channel dynamics, sediment transport, and the slope of alluvial fans: experimental study. The Journal of Geology 106(6):677–694

Yin SL, Wu SH, Feng W j, Li JF, Yin H (2013) Patterns of intercalation in alluvial fan reservoirs—a case study of Lower Karamay Formation, Yizhong Area, Karamay Oilfield, NW China. Pet Explor Dev 40(6): 811–818

Zhang T, Zhang X, Lin C, Yu J, Zhang S (2015) Seismic sedimentology interpretation method of meandering fluvial reservoir: from model to real data. J Earth Sci 26(4):598–606

Zhang X, Wang S, Wu X, Xu S, Li Z (2016) The development of a laterally confined laboratory fan delta under sediment supply reduction. Geomorphology 257:120–133